

Cite this: *Polym. Chem.*, 2026, **17**,
1661

Recent progress in bulk polymerization: spatiotemporally discontinuous change of polymerization accompanied by phase separation

Yasuhito Suzuki * and Akikazu Matsumoto

Bulk polymerization converts liquid monomers into polymeric materials through an exothermic reaction, often leading to vitrification or the formation of highly viscous polymer melts depending on the monomer chemistry. It has long been assumed *a priori* that the polymerization solution remains homogeneous throughout the reaction process. Recent advances have revealed that apparent phase separation takes place near the polymerization-induced vitrification, and this event is closely linked to sudden reaction acceleration (*i.e.*, the Trommsdorff effect) during bulk polymerization. Insights from recent studies on amorphous structure evolution have provided new perspectives on how local heterogenization affects reaction kinetics. This review summarizes recent progress in understanding bulk polymerization, with a focus on sudden reaction acceleration, and discusses the potential outcomes of the novel view.

Received 5th January 2026,
Accepted 10th April 2026

DOI: 10.1039/d6py00006a

rsc.li/polymers

1. Introduction

Bulk polymerization, defined as polymerization conducted without intentionally added solvent, represents one of the most fundamental reaction schemes in polymer chemistry. Owing to its apparent simplicity, bulk polymerization has long been described within a homogeneous reaction framework, in which conversion, viscosity, and heat generation are assumed to evolve uniformly throughout the reaction medium.¹ This assumption has provided the basis for classical interpretations of reaction kinetics and has been widely adopted in both academic textbooks^{1–3} and industrial practice. However, it has become increasingly clear that this homogeneous picture is frequently oversimplified, particularly in bulk polymerizations that undergo drastic changes in physical properties during the reaction.^{4–7} In highly exothermic chain-growth polymerizations, strong coupling among reaction kinetics, heat transfer, diffusion, and polymerization-induced vitrification occurs in conjunction with spatial and temporal inhomogeneities.^{8,9} These findings motivate a re-examination of bulk polymerization from a spatiotemporally heterogeneous viewpoint.

Fig. 1 provides a conceptual classification of bulk polymerization based on reaction mechanism, spatial confinement, and spatiotemporal uniformity during polymerization. The reaction mechanism can be chain-growth (*i.e.*, radical or

ionic), step-growth, or ring-opening polymerization. With respect to spatial organization, polymerization may proceed in a homogeneous bulk system or in heterogeneous forms such as suspension, emulsion, or precipitation polymerization. Here we would like to define terms. “Heterogeneous polymerizations” refer to systems in which polymerization proceeds within physically separated reaction domains, such as droplets or particles defined by interfaces. Unless we explicitly state “heterogeneous polymerizations”, we define the term heterogeneity referring to a concentration fluctuation on a nanometer scale that is intimately related to the chemical reaction kinetics. When the heterogeneity grows on a larger scale, we use the term phase separation. Such nanoscale heterogeneity may evolve into larger domains during polymerization, eventually becoming observable as apparent phase separation. In a strict thermodynamic sense, phase separation refers to the spontaneous demixing of a homogeneous system into coexisting phases driven by a free-energy instability. When chemical reactions such as polymerization are involved, however, the system is inherently out of equilibrium, and spatial segregation controlled or even triggered by reaction kinetics cannot be excluded. In such cases, the term “phase separation” is often used in a broader, phenomenological sense to describe spatial segregation that does not necessarily correspond to an equilibrium phase boundary. Similar concepts have attracted wide attention in other fields, most notably in biology, where liquid–liquid phase separation in cells is now recognized as a general organizing principle involving nonequilibrium and transient states.¹⁰ This distinction is particularly useful for discussing bulk polymerization, where subtle heterogeneity emer-

Department of Applied Chemistry, Graduate School of Engineering, Osaka Metropolitan University, 1-1, Gakuen-cho, Naka-ku, Sakai, Osaka 599-8531, Japan.
E-mail: suzuki_y@omu.ac.jp





Fig. 1 Conceptual framework of polymerization and the emergence of heterogeneity in bulk polymerization. Polymerization reactions are classified by mechanism (radical, ionic, step-growth, and ring-opening), and polymerization systems are categorized by spatial organization (bulk, suspension, emulsion, and precipitation). While bulk polymerization has traditionally been regarded as homogeneous, strong coupling among reaction kinetics, diffusion, and vitrification leads to the emergence of spatiotemporal heterogeneity, often associated with the Trommsdorff effect. Representative modes of spatiotemporal organization in bulk polymerization are illustrated, including uniform reaction, nanoscale heterogeneity characterized by monomer-rich and polymer-rich regions, and frontal polymerization involving a propagating reaction front.

ging at the nanoscale can strongly affect molecular mobility and reaction kinetics, ultimately leading to sudden reaction acceleration and, in extreme cases, to propagating reaction fronts. Based on this framework, this review aims to provide a unified perspective on bulk polymerization by integrating classical concepts with recent experimental advances. Special emphasis is placed on the interplay among polymerization-induced vitrification, heterogenization, and reaction kinetics, with a focus on understanding the molecular origin of sudden reaction acceleration known as the Trommsdorff effect and its connection to spatiotemporally heterogeneous polymerization processes. Recently, a special case of bulk polymerization, namely frontal polymerization, has attracted considerable attention.¹¹ In this polymerization method, the reaction is triggered locally at a specific point, and the polymerization proceeds in a spatially confined manner. The polymerized region then propagates through the material with a well-defined reaction front. Because this method utilizes the heat generated by the polymerization reaction, it is an energy-efficient process. Although frontal polymerization has a long history and great potential, not all monomers allow smooth and well-controlled curing.¹² A better understanding of bulk polymerization is therefore key to achieving reliable control of frontal polymerization. In this review, we also discuss the perspectives underlying the control of frontal polymerization.

2. Categories of bulk polymerization

2.1 Bulk polymerization

In chemistry, solvents are often used, and the polymerization in a solvent is called solution polymerization. On the other hand, polymerization without solvent is termed bulk polymerization. Typically, a small amount of initiator is dissolved in monomer, and a reaction is initiated. Polymerization methods can be categorized into chain-growth polymerization and step-growth polymerization. In principle, bulk polymerization can be applied to any polymerization method, provided that the initiator is soluble in the monomer or that a stimulus can initiate the reaction. There are several motivations for using bulk polymerization. One key reason is its suitability for resin curing, and another is its synthetic advantages, including the avoidance of solvents and the ability to achieve higher conversion rates.

When the glass transition temperature of the resulting polymer exceeds the reaction temperature, polymerization typically yields a glassy solid from a liquid monomer. As the reaction progresses, viscosity generally increases. Whether the resin vitrifies is a critical characteristic for curing. Heterogeneity in polymerizing systems has also been widely discussed in the context of crosslinking polymerizations, where intramolecular cyclization and early network formation



can lead to the formation of microgel-like structures and spatially heterogeneous networks. Such microgel formation processes have been extensively investigated in classical studies of crosslinking radical polymerizations.^{13–16} In contrast, the present review focuses on heterogeneity emerging during bulk polymerization of linear polymers, particularly near vitrification, where spatial heterogeneity develops dynamically as a result of the coupling between reaction kinetics, diffusion, and glass transition. In this review, we focus on bulk radical polymerization and bulk ring-opening polymerization, both of which lead to vitrification, exploring their fundamental principles and practical applications. While heterogeneity can also arise in other classes of polymerization reactions, including step-growth polymerizations and controlled/living radical polymerizations, the present review focuses primarily on chain-growth systems. These systems most prominently exhibit strong spatiotemporal heterogeneity during bulk polymerization because monomer and polymer species coexist with markedly different dynamical properties. As polymerization proceeds, the increasing contrast between the fast dynamics of monomers and the slow segmental dynamics of growing polymer chains gives rise to pronounced dynamic heterogeneity, particularly as the system approaches vitrification. In step-growth polymerizations, molecular weight increases gradually and high-molecular-weight species appear only at very high conversion. Consequently, the dynamical contrast between monomeric and polymeric species remains relatively small during most of the reaction, and the development of strong spatiotemporal heterogeneity is less pronounced compared with chain-growth systems. In addition, controlled/living radical polymerizations often suppress termination reactions and proceed under conditions where the concentration of active species remains extremely low, which may reduce the likelihood of sudden kinetic acceleration associated with the Trommsdorff effect. The term curing is loosely defined in polymer chemistry. It is often used when a liquid turns into a glassy or semi-crystalline solid. In some cases, they use the term only for thermosets. In this review, we use the term curing irrespective of whether the resin is thermoplastic or thermoset.

2.2 Bulk radical polymerization

Bulk radical polymerization is widely applied in many fields. A small amount of radical initiator is mixed with the monomer. In most cases, initiation is triggered by heat, but it can also be initiated by light irradiation with an appropriate photoinitiator. Radical polymerization has several key characteristics. Firstly, the radical concentration is significantly lower than that of the monomer, typically by a factor of 10^{-8} .¹⁷ Secondly, the lifetime of radicals is extremely short, usually on the order of 100 microseconds.¹⁸ This short lifetime allows for the rapid formation of high-molecular-weight polymer chains. As a result, the process can be viewed as a relative change in concentration between monomers and polymers. When the reaction temperature is below the glass transition temperature of the formed polymer, polymerization-induced vitrification is

expected. Thirdly, reactive monomers are highly exothermic. Polymerization is entropically unfavorable due to the loss of degrees of freedom; thus, the process must be enthalpically driven. For instance, the heats of the reaction for MMA (methyl methacrylate) and MA (methyl acrylate) are 55 and 78 kJ mol⁻¹, respectively.¹⁹ This highly exothermic nature can lead to thermal runaway.

2.3 Bulk ring-opening polymerization

Ring-opening polymerization involves the conversion of cyclic monomers into linear polymer chains. Polymerization is generally entropically unfavorable because the formation of covalent bonds reduces the freedom of polymer chains to explore configurational space, leading to a decrease in entropy. The reaction can nevertheless proceed because the enthalpic gain associated with bond formation compensates for the entropy decrease. In ring-opening polymerization, the enthalpic gain from ring-strain release can further drive the reaction, and the balance between enthalpy and entropy may lead to monomer–polymer equilibria depending on the monomer structure and temperature.^{1,20} Another advantage of ring-opening polymerization is the relatively small change in density. Therefore, the formation of voids may be low. Therefore, the potential application for reactive processing has been proposed.²¹ Epoxy resins are also categorized as ring-opening polymers. Since there are already a number of reviews,^{22,23} we will not discuss this topic in this manuscript. Recently, ring-opening metathesis polymerization^{24,25} (ROMP) has attracted much attention due to its potential for application. Olefin metathesis is an organic reaction in which the fragments of alkenes (olefins) are redistributed through the breaking and reforming of carbon–carbon double bonds. Although studies on bulk ring-opening polymerization under conditions comparable to those discussed for radical polymerization are still limited, similar kinetic phenomena may occur. In particular, the possibility that reaction-induced heterogeneity could lead to Trommsdorff-like rate acceleration in bulk ring-opening systems remains an interesting open question.

3. Reaction-induced vitrification and heterogenization

3.1 Homogeneous view and heterogeneous view

Because the Trommsdorff effect is closely related to vitrification and heterogeneity, we first discuss the structural evolution during polymerization before describing the kinetic aspects in section 4. It has long been assumed *a priori* that the polymerization solution remains homogeneous throughout the bulk polymerization process. In chain-growth bulk polymerization, the relative concentrations of monomer and polymer change as the reaction proceeds. From a simplified perspective, macroscopic viscosity is a key parameter for understanding the changing physical properties of the polymerization solution. However, the relationship between polymer fraction and macroscopic viscosity is complex. In addition to these well-



studied aspects of polymer solution dynamics, the polymerization solution eventually vitrifies, becoming a glassy solid as long as the polymer's glass transition temperature exceeds the reaction temperature. It should be noted that, in crosslinking radical polymerizations, structural heterogeneity associated with gelation and microgel formation has long been recognized. Early studies on controlled radical copolymerization of vinyl/divinyl monomers provided important mechanistic insights into gelation behavior.²⁶

3.2 Polymerization-induced apparent phase separation

Wöll *et al.* investigated bulk polymerization using single-molecule spectroscopy^{4,5,27} and observed that the dynamics of single molecules became heterogeneous at a certain point during the bulk polymerization of MMA. Initially, the dye dynamics were unimodal, but they suddenly became bimodal, with some dye molecules moving rapidly while others moved slowly, as depicted in Fig. 2. Interestingly, this shift coincided with the reaction acceleration known as the Trommsdorff effect. In contrast, the distribution of the dynamics of the dye remains unimodal during bulk polymerization of styrene. While it has been known that the Trommsdorff effect is observed from styrene, the degree of the effect is much smaller than that of MMA.²⁸

Later studies using video recordings revealed that the polymerization solution becomes discontinuously hetero-

geneous at the onset of the Trommsdorff effect. Apparent phase separation was observed, partially due to the coloration caused by amines used in the redox reaction for initiation.⁹ Fig. 3 shows selected photographs during the bulk polymerization of MMA. Both MMA and PMMA are transparent. However, their refractive indices are different. Nanoscale heterogeneity may initially emerge during polymerization and, under certain conditions, evolve into larger domains. Once the characteristic length scale becomes sufficiently large, light scattering increases and the system appears opaque. At around 70 minutes after the initiation, the top part of the polymerization solution becomes white. This time is in good agreement with the onset of the sudden temperature rise. Subsequently, at around 100 minutes, the white region also appears in the middle of the polymerization solution. Further investigations using transmission measurements confirmed that this apparent phase separation is observed universally with azo initiators.^{8,17} After the reaction completes, a distinct boundary between the two phases remains visible, even though both layers are composed of PMMA. This boundary disappears only after annealing above the glass transition temperature. The correlation between the Trommsdorff and the phase separation is also pointed out in a study that intentionally caused phase separation.^{29,30} Recently, the liquid-liquid phase separation in a living cell has attracted many researchers because it may play vital roles in governing the chemical reactions in



Fig. 2 Distribution of diffusion coefficients obtained from single-molecule spectroscopy for styrene (left) and MMA (right). Reproduced from ref. 6 with permission from the Royal Society of Chemistry, *Polym. Chem.*, 2012, 3, 2456–2463, copyright 2012.





Fig. 3 Selected photographs (a–o) taken at different times during the bulk polymerization of MMA. A white region due to macroscopic apparent phase separation can be observed. The timing of the phase separation coincides with the onset of the Trommsdorff effect. Reproduced from ref. 9 with permission from Springer Nature, *Polym. J.*, 2019, **51**, 423–431, copyright 2019.

living cell.^{10,31–33} In a living cell, the phases are inherently not only governed by thermodynamics but also by kinetics.

Microscopic heterogeneity was further confirmed using small-angle neutron scattering (SANS).³⁴ Repeated SANS measurements over small-angle q -ranges, taking approximately five minutes per scan, captured a discontinuous change during the bulk polymerization of MMA. This change coincided with the onset of the Trommsdorff effect. It revealed that concentration fluctuations steadily decreased before the Trommsdorff effect but increased discontinuously from approximately 2 nm to approximately 5 nm at its onset. These findings suggest that the polymerization solution becomes microscopically heterogeneous, leading to macroscopic apparent phase separation.

3.3 Polymerization-induced vitrification

As mentioned earlier, polymerization-induced vitrification (*i.e.*, glass transition) occurs during bulk polymerization when the reaction temperature is lower than the glass transition temperature of the resulting polymer. Recent studies on amorphous materials suggest that the packing of amorphous structures, as determined by the vitrification process, significantly affects their physical properties. A representative example is vapor-deposited glass.³⁵ Despite its importance both in fundamental science and applications and tremendous work, the fundamental mechanism of glass transition is still elusive.³⁶ The importance of spatiotemporal heterogeneity has been pointed out.³⁷ While glass transition is often discussed in the context of temperature changes, it can also occur due to pressure or compositional changes.³⁸ For instance, relative concentration changes can result from chemical reactions or solvent evaporation. Vitrification caused by compositional changes is known to play a significant role in atmospheric and

food sciences. Recent *in operando* SAXS/XPCS on a commercial two-component MMA adhesive directly visualized nm-scale domain growth, gel-point percolation-like behavior, and a “long-tailed” vitrification regime persisting far beyond macroscopic gelation. Importantly, this late-stage vitrification dominated the final mechanical properties, demonstrating a clear process–structure–dynamics–property link under industrially relevant curing conditions.³⁹

There are several experimental approaches to studying vitrification induced by relative concentration changes. One classical method involves dissolving a polymer in a solvent and increasing the polymer concentration. However, the dissolution kinetics of polymers are generally very slow, because the solvent must first penetrate the polymer’s glassy matrix before the entangled polymer chains can be released.⁴⁰ As the polymer concentration increases, the dissolution process becomes even slower, making it difficult to prepare highly concentrated polymer solutions close to vitrification. Another approach is to increase the polymer concentration through solvent evaporation. In such systems, however, solvent evaporation often leads to the formation of a dense skin layer at the surface, which suppresses uniform concentration changes in the bulk.⁴¹ In this context, bulk polymerization can be seen as polymerization-induced vitrification when the reaction temperature is below the glass transition temperature of the formed polymer.⁴² As discussed, the concentration of the existing radicals is negligibly small in comparison to the concentrations of monomers and polymers. Once a radical is generated, a polymer with reasonable molecular weight is formed within a very short time. Therefore, in a rough approximation, bulk polymerization can be seen as a process where the relative concentration of monomer and polymer changes as the reaction proceeds. A recent study investigated the bulk polymerization of MMA using dielectric spectroscopy.⁸ Fig. 4 shows the profile of dielectric spectroscopy and the temperature profile during the measurement. After the disappearance of the α relaxation, a hidden, smaller process (*i.e.*, the β relaxation process) appeared. The characteristic time of the β relaxation process does not change significantly upon polymerization reaction, suggesting the local character of this relaxation process. Essentially, this observation captured the polymerization-induced vitrification.³⁸ While most of these studies have been conducted using MMA, similar results have also been reported for EMA and BMA.⁴³

3.4 Changes in amorphous structures during curing

The glass transition remains one of the most significant and challenging unsolved problems in condensed matter physics.³⁶ While its fundamental nature is still under debate, understanding of glass and the glass transition has advanced significantly through solid experimental results.^{44–46} Amorphous structures can be analyzed using X-ray scattering, with pair distribution function (PDF) analysis often employed to investigate real-space structures.^{47,48}

The amorphous structure of polymers has been studied extensively. A broad scattering intensity profile, referred to as





Fig. 4 (a) Dielectric spectra recorded during the bulk polymerization of MMA at 40 °C. Each curve corresponds to a successive measurement taken as the polymerization proceeds. The α -relaxation peak shifts from higher to lower frequencies and eventually moves out of the experimental window. The arrow indicates the shift of the main peak during the reaction. After the main peak disappears, a smaller peak becomes visible. (b) Corresponding temperature profile showing a small but noticeable temperature increase occurring near the divergence of the α -relaxation. Reproduced from ref. 8 with permission from the American Chemical Society, *Macromolecules*, 2021, **54**, 3293–3303, copyright 2021.

the amorphous halo, is typically observed. Despite efforts to elucidate the structure and understand the physical properties of amorphous polymers, extracting detailed information from their X-ray scattering profiles remains challenging. Recent studies have reported changes in the amorphous structure during the bulk polymerization of MMA, EMA, and BMA.

Although it is difficult to directly correlate physical properties with amorphous structures, tracking these changes provides valuable insights into resin-curing mechanisms.

Fig. 5 displays the amorphous structure of monomer and polymer, as well as the changes in amorphous structure during bulk polymerization.⁴⁹ Notably, the transition in amor-



Fig. 5 Amorphous structures measured by X-ray scattering during the bulk polymerization of MMA, EMA, and BMA. The initial (mainly monomer) and final (mainly polymer) structures are shown for (a) MMA, (b) EMA, and (c) BMA. The full datasets obtained during the bulk polymerization of MMA, EMA, and BMA are presented in (d), (e), and (f), respectively. Reproduced from ref. 42 with permission from Springer Nature, *Polym. J.*, 2023, **55**, 807–815, copyright 2023.



phous structure is not smooth. Initially, the structure closely resembles that of the pure monomer, with the peak position of the amorphous halo remaining nearly unchanged. As the polymer fraction increases, the peak broadens. At a certain point during bulk polymerization, a sudden shift occurs, transitioning from a monomer-like structure to a polymer-like structure. This change coincides with the reaction acceleration known as the Trommsdorff effect. The difference between the amorphous structures of monomer and polymer is more pronounced in BMA than in MMA, likely due to BMA's longer side chains. In monomers, the side chains exhibit a high degree of freedom, but during polymerization, they become more ordered. This ordering is considered to be associated with enhanced intermolecular correlations of the side chains, which manifests as a relatively sharp peak in the amorphous halo at lower q ranges.

4. Reaction kinetics during bulk polymerization

4.1 A sudden reaction acceleration during bulk polymerization (Trommsdorff effect)

It has long been known that sudden reaction acceleration can occur during bulk radical polymerization, a phenomenon often referred to as the Trommsdorff effect.¹ This effect is particularly prominent during the bulk polymerization of methyl methacrylate. Although methacrylates have been the most extensively studied systems, systematic investigations of bulk radical polymerization remain limited for many other monomers. As a result, it is not always clear whether similar sudden reaction acceleration occurs universally across different monomer systems or under what conditions it emerges. Fig. 6 shows the conversion and temperature profile during the bulk polymerization of methyl methacrylate. However, at approximately 80 minutes when the initial initiator concentration is 6 wt%, the temperature rises dramatically from 50 °C to 83 °C within just 5 minutes. Classically, this effect has been attributed to a decrease in the termination rate caused by the increased viscosity of the reaction medium.¹ However, the abruptness of the effect suggests that increased viscosity alone cannot fully explain its occurrence. The molecular origin of the Trommsdorff effect remains a subject of ongoing debate and investigation.

Another important feature of the Trommsdorff effect is the distinct change in the formed molecular weight.^{8,9,30,50} Fig. 7 shows the molecular weight distribution as a function of reaction time during bulk polymerization of MMA. At the onset of the Trommsdorff effect, the formed molecular weight changes discontinuously. It is noted that this change occurs suddenly within a short time, implying a discontinuous change in the reaction kinetics.

4.2 History of the research on the Trommsdorff effect

The sudden reaction acceleration, known as the Trommsdorff effect, was first observed by Norrish and Brookman in 1939.⁵¹

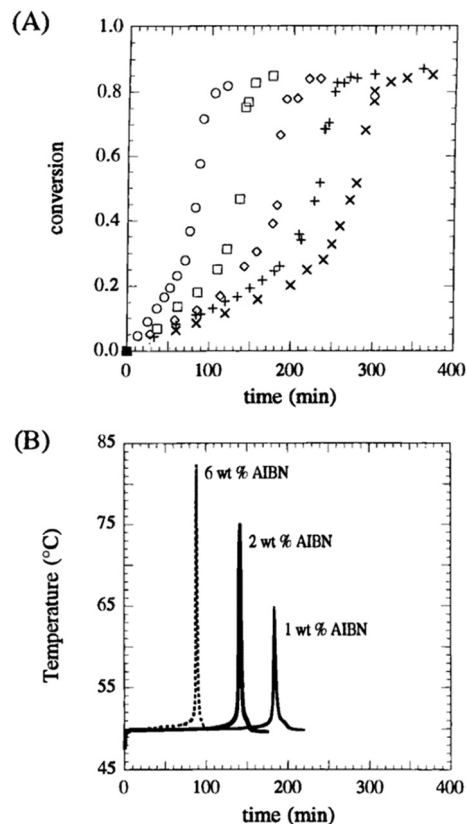


Fig. 6 (A) Conversion profile and (B) temperature profile during the bulk polymerization of MMA. Symbols correspond to initiator concentrations of 6 wt% (○), 2 wt% (□), 1 wt% (◇), 0.5 wt% (+), and 0.3 wt% (×). Reproduced from ref. 67 with permission from the American Chemical Society, *Macromolecules*, 1996, 29, 7477–7490, copyright 1996.



Fig. 7 Time-resolved molecular weight of PMMA during the bulk polymerization under light irradiation for different durations. Reproduced from ref. 30 with permission from Elsevier, *Polymer*, 2014, 55, 1809–1816, copyright 2014.



According to kinetic theory, the rate of radical polymerization (R_p) obeys the following equation:

$$R_p = k_p[M](2f/k_d[I]/k_t)^{1/2} \quad (1)$$

Here, k_p , k_d , and k_t are propagation rate, decomposition rate, and termination rate, respectively. $[M]$, $[I]$ and f are monomer concentration, initiator concentration, and initiator efficiency, respectively. In 1942, they proposed that this effect occurs due to the decrease in termination rate.⁵² This phenomenon was further analyzed by Trommsdorff, who concluded that the effect is due to a decreased termination rate in 1948.⁵³ As the reaction proceeds, the viscosity of the reaction medium increases due to the formation of highly viscous polymers. High viscosity reduces molecular mobility, making it difficult for two high-molecular-weight radicals to collide and undergo termination. In contrast, monomer molecules, being smaller, can still move relatively freely, allowing propagation to continue. Thus, while increased viscosity significantly slows the termination reaction, its impact on the propagation rate is limited. As a result, the overall reaction rate increases dramatically (Fig. 8). Similar conclusions are drawn in the same period by different scientists.^{54–56} This explanation is also documented in Paul Flory's textbook on polymer chemistry.¹ In the textbook, Flory discusses this phenomenon carefully and avoids a definitive conclusion. Recent textbooks essentially follow this classical explanation.^{2,3,57,58}

The explanation based on the reduced termination rate due to the increased viscosity sounds qualitatively reasonable.

There are several studies investigating the propagation rate and the termination rate.^{59–61} The sudden decrease in termination rate at the late stage of bulk polymerization has been captured by ESR experiment.⁶¹ A more detailed analysis of the rate constants in radical polymerization is still ongoing.^{62,63} On the other hand, it has been realized that this explanation does not quantitatively explain the actual experimental data. For example, the onset of the Trommsdorff effect cannot be reasonably predicted. In 1981, Tirrell *et al.* approached this problem from the polymer physics aspect.⁶⁴ They proposed that the onset of the Trommsdorff effect occurs due to the entanglement of the polymer chains. At that time, many researchers actively investigated the entanglement of polymer chains inspired by earlier works by De Gennes⁶⁵ and later by Doi and Edwards.⁶⁶ It was shown that the Trommsdorff effect is still present⁶⁷ without entanglement. In order to entangle, the molecular weight of the polymer needs to be high. They used a chain transfer agent to control the molecular weight of the formed polymer. Even when the molecular weight of the formed polymer is below the entanglement molecular weight, they observed the Trommsdorff effect. Other research also supports the uncorrelation between entanglement and the Trommsdorff effect.⁶⁸ After the 1990s, studies using computer simulation started. If the decrease in termination rate is the reason for the Trommsdorff effect, the effect can be predicted by the coupled differential equations describing the reaction kinetics.^{28,69–71} Many scientists proposed models taking into account the decrease in termination rate due to the increased viscosity. As a result, the widely used model uses four different



Fig. 8 Classical explanation of the Trommsdorff effect. As viscosity increases, both the propagation rate constant (k_p) and the termination rate constant (k_t) decrease because molecular motion is suppressed. The decrease in k_t is greater than that in k_p , since monomer molecules can still move even at high viscosity, whereas termination requires the encounter of two radical chain ends. Consequently, propagation becomes relatively favored, leading to the Trommsdorff effect. However, macroscopic viscosity alone is insufficient to quantitatively describe its onset.



sets of differential equations.⁷² They switch these functions based on the experimental data. In other words, the mathematical model is empirical and cannot be used for prediction.

Norrish and Smith proposed that the effect is due to the decreased termination rate in 1942.⁵² In 1948, Trommsdorff published a systematic research on this topic and concluded that the effect is due to the decreased termination rate due to the increased viscosity.⁵³ It is difficult to select whose name to use to describe this effect.^{73–76} This phenomenon has been described by several terms in the literature, including the Trommsdorff effect, the Trommsdorff–Norrish–Smith effect, the gel effect, and autoacceleration. In this review, we use the term Trommsdorff effect, which is currently the most widely used designation. Instead of the terms from scientists' names, the term gel effect is often used. If the effect is due to the entanglement, this term is reasonable because the entanglement can be seen as a physical crosslinking. Since it is now considered that the effect and the entanglement do not coincide, we think the term gel effect may not be suitable. In addition, the term autoacceleration is occasionally used to describe this effect. It is true that the positive feedback is present when this effect takes place. Due to the increased overall kinetics, the temperature increases. The increased temperature further increases the overall kinetics.

4.3 A novel view on the Trommsdorff effect in conjunction with heterogenization

4.3.1 Key observation: discontinuous heterogenization coincides with autoacceleration. A key experimental observation in bulk methacrylate polymerization is that the onset of the Trommsdorff effect coincides with the emergence of spatial heterogeneity. Experimental studies using optical observation, scattering techniques, and spectroscopic methods have shown that the polymerizing system undergoes a discontinuous change in its spatial structure during the late stage of the reaction. This transition is accompanied by the appearance of polymer-rich and monomer-rich regions and occurs near the point where the polymerization rate increases sharply. These observations suggest that the Trommsdorff effect is closely linked to the development of heterogeneity in the polymerization medium.

4.3.2 What changes kinetically: termination suppressed vs. propagation maintained/enhanced. The imbalance between the decreased termination rate and the relatively stable propagation rate leads to a sudden increase in reaction acceleration. However, as mentioned earlier, there is a discrepancy between experimental data and the expected changes in macroscopic viscosity. The Trommsdorff effect occurs so abruptly and almost discontinuously that the increase in viscosity alone cannot fully explain it. Polymerization-induced heterogenization or apparent phase separation can be a candidate that triggers the Trommsdorff effect. In the classical view of the Trommsdorff effect, the main cause is the probability of meeting two molecules involved in the reaction. In the case of the termination reaction, it was the two radicals. In the case of

the propagation reaction, it was the radical and the monomer. The rate parameters (k_i) for chemical reactions follows the Arrhenius equation as depicted in eqn (2).

$$k_i = k_0 \cdot \exp\left(-\frac{E_a}{RT}\right) \quad (2)$$

Here, k_0 , E_a , R and T denote the frequency parameter, activation energy, gas constant, and temperature, respectively. It is evident that the reaction rate depends on temperature. Catalysts or enzymes in biological systems reduce the activation energy to govern chemical reactions. On the other hand, the effect of the pre-exponential factor (*i.e.*, the frequency parameter) is often overlooked. The frequency parameter reflects the probability of two chemical species meeting during the reaction. In a large solvent volume, it is reasonable to assume that the frequency factor remains constant.

4.3.3 Mechanistic picture: radicals partition to polymer-rich domains/interfacial reaction. In the case of the Trommsdorff effect, changes in the frequency factor have been considered. These changes are influenced not only by macroscopic viscosity but also by microscopic heterogeneity at various length scales. When the amorphous structure of the polymerization solution changes, the frequency factor may also be affected through changes in local molecular arrangements.⁴² At a slightly larger scale, microscopic phase separation creates monomer-rich and polymer-rich phases. Radicals likely tend to exist in the polymer-rich phase. Depending on the domain size and the dynamics of radicals, the probability of two radicals meeting may decrease. However, since monomers remain in the low-viscosity monomer-rich phase, the probability of a radical meeting a monomer does not decrease and may even increase.

This increase can occur for two reasons. First, depending on molecular arrangement, the likelihood of radicals meeting monomer molecules may rise. Second, chemical reactions at the molecular level induce changes in chemical potential. At low viscosity, the gradient of chemical potential quickly dissipates. In contrast, at higher viscosity, the gradient persists longer, allowing monomers to move along it. This could lead to a more efficient supply of monomers to radicals.

As shown in photographs of bulk-polymerized samples in vials, macroscopic heterogeneity develops on a millimeter-to-centimeter scale. This observation suggests the formation of a propagating reaction interface between polymer-rich and monomer-rich regions. Such behavior may be interpreted as a front-like propagation mode of polymerization, which may involve the coupling between reaction kinetics, diffusion, and polymerization-induced heterogeneity. In addition, experimental observations indicate that multiple interfaces can appear and subsequently merge during the course of polymerization, suggesting that the spatial discontinuity cannot be explained solely by a simple oxygen inhibition gradient but instead reflects the intrinsic coupling between reaction kinetics, diffusion, and polymerization-induced heterogeneity. Under such conditions, the frequency factors for termination



and propagation reactions likely differ from those in a homogeneous polymerization solution. Recent *in situ* observations using ultrasonic detection⁷⁷ and SANS/WAXS⁷⁸ directly captured the formation of monomer-rich and polymer-rich domains, reinforcing the heterogenization-driven view of the Trommsdorff effect. Although the detailed molecular mechanisms remain unclear, changes in the frequency parameter due to polymerization-induced heterogeneity may provide a possible explanation for the Trommsdorff effect. These observations suggest that late-stage bulk methacrylate polymerization is not well described as a spatially uniform reaction. Once monomer-rich and polymer-rich regions emerge, radicals are expected to localize in the polymer-rich phase, and reactions proceed preferentially at interfaces, potentially leading to front-like propagation behavior. In this sense, frontal polymerization can be viewed as an extreme manifestation of the same heterogeneity–kinetics coupling discussed above. More broadly, such reaction-induced heterogeneity may provide a conceptual link to nonequilibrium phase-separation phenomena observed in other complex chemical systems, including liquid–liquid phase separation in biological environments. A classical MMA/PMMA system already illustrates that a visible interfacial front can propagate even near room temperature: polymerization initiates in a swollen polymer layer acting as a microreactor, and the rate enhancement in this viscous region—attributed to the Trommsdorff effect—constitutes the actual origin of the frontal polymerization.⁷⁹ It has also been reported that the presence of polyethylene glycol enhances the polymerization kinetics of MMA.^{80–82} This could also be explained by the reaction acceleration due to heterogeneity.

5. Applications of bulk polymerization

5.1 Frontal polymerization

Frontal polymerization provides an illustrative example of how strong coupling between reaction kinetics, heat and mass transport, and spatial heterogeneity can lead to the formation of a propagating reaction front. Because chain formation reduces molecular degrees of freedom ($\Delta S < 0$), the enthalpy change must be sufficiently negative to compensate for this entropy loss and ensure that $\Delta G < 0$. For this reason, bulk polymerization of vinyl monomers is generally exothermic. In radical polymerization of vinyl monomers, this heat release can be substantial ($\Delta H \approx 50\text{--}80 \text{ kJ mol}^{-1}$).¹⁹ Frontal polymerization refers to a mode of polymerization in which a localized reaction zone propagates through the material. Depending on the driving mechanism, frontal polymerization is generally classified into thermal frontal polymerization and isothermal frontal polymerization.⁸³ In thermal frontal polymerization, the propagation of the reaction front is sustained by the heat released during the exothermic polymerization reaction. The heat generated at the reaction front diffuses into the surrounding monomer and triggers further polymerization, allowing the front to propagate without continuous external heating.⁸⁴

This concept of a self-sustaining polymerization front was established in early studies and has since been extensively investigated.^{85–87} In contrast, isothermal frontal polymerization occurs without relying on thermal feedback. Early experimental observations related to such front-like propagation in MMA-based systems were reported in interfacial-gel copolymerization used for graded-index polymer optical waveguides.⁸⁸ Similar propagation behavior was also utilized in the fabrication of graded-index plastic optical fibers.⁸⁹ Later studies explicitly described non-thermal frontal polymerization of MMA in systems containing polymeric seeds modified with metal–porphyrin complexes.⁹⁰ The influence of reaction conditions on such front propagation was subsequently investigated in detail.⁹¹ Further studies examined the role of polymer inhibitors in controlling the propagation behavior.⁹² Mechanistic aspects of isothermal frontal polymerization and factors governing front velocity and propagation distance have also been investigated experimentally and theoretically.⁸³ In particular, the role of oxygen inhibition and the molecular weight of polymer seeds has been shown to significantly influence the stability of the propagating front.⁹³ In this case, a localized high-viscosity reaction zone is formed in a polymer-rich region, and diffusion of monomer and initiator into this region induces strong rate acceleration associated with the Trommsdorff effect. As a result, polymerization can propagate along the interface between polymer-rich and monomer-rich regions even under nearly isothermal conditions. This phenomenon has been mainly reported for methyl methacrylate-based systems and has been investigated in several experimental and theoretical studies. Although thermal and isothermal frontal polymerization are often classified separately according to their dominant driving mechanisms, both involve strong coupling between reaction kinetics, transport processes, and spatial heterogeneity, although their dominant driving mechanisms are different.

At the bottom of the vial, PMMA seed is prepared. The addition of monomer with the initiator dissolves PMMA. At the dissolved layer, the Trommsdorff effect takes place as the polymer concentration is high. Therefore, the front propagation occurs, leading to frontal polymerization of MMA. Efficient utilization of the generated heat enables self-sustaining curing, providing the basis for frontal polymerization, in which the polymerization front propagates through the material without continuous external heating. This process can be regarded as a spatial manifestation of polymerization-induced heterogeneity. While thermal transport and heat balance remain central to frontal polymerization, accumulating evidence indicates that polymerization-induced heterogeneity and local kinetic acceleration analogous to the Trommsdorff effect can play a decisive role, particularly in methacrylate-based systems. Beyond kinetic interest, frontal polymerization has been exploited as a rapid and energy-efficient route to fabricate monolithic macroporous polymers, where a localized polymerization zone is synchronized with foaming to generate porous structures without relying on large volumes of organic solvent or high-pressure equipment.⁹⁴



Frontal polymerization was first explored in the 1970s and has since been comprehensively reviewed.¹² The key factor governing front propagation is the heat balance between generation and dissipation, which depends on monomer reactivity, initiator concentration, and thermal transport. In practice, however, voids and cracks often form because of density and viscosity differences between the monomer and polymer phases, limiting the fabrication of large parts. Understanding the interplay between thermal transport and local heterogeneity is therefore essential for expanding frontal polymerization to advanced manufacturing applications. Frontal ring-opening metathesis polymerization (FROMP) has attracted considerable attention from many researchers. In particular, FROMP of norbornene derivatives provides a promising route for the fabrication of polymer components.⁹⁵ The major advantage of ring-opening polymerization is the minimal change in density during the course of polymerization. In addition, polymers obtained from norbornene derivatives exhibit excellent mechanical and thermal properties.

5.2 Resins for fiber-reinforced plastics

Fiber-reinforced plastics are an important application area of bulk polymerization processes.

Because the curing of these resins often proceeds through highly viscous states accompanied by polymerization-induced vitrification and strong reaction-transport coupling, they provide practical examples where the phenomena discussed in the previous sections become technologically relevant. Due to their strength and lightweight, fiber-reinforced plastics span their application area.^{96–98} Carbon fiber-reinforced plastics are used in advanced technology for airplanes and sports utilities, whereas glass fiber-reinforced plastics are used for wind turbine blades. Generally, thermosets, including epoxy resin



Fig. 10 Demonstration of fiber (bottom left) and polymer (bottom right) recovery by dissolution from a glass-fiber-reinforced composite (top) using Elium as the resin. Reproduced from ref. 102 with permission from Elsevier, *J. Cleaner Prod.*, 2019, **209**, 1252–1263, copyright 2019.

and unsaturated polyurethanes, are used. The use of thermosets requires post-curing and annealing. In addition, the drawback of thermosets is the difficulty of recycling.

For the composite fabrication, the viscosity of the resin plays a crucial role. Fig. 9 summarizes viscosity as a function of processing temperature.²¹ The melt processing requires high temperature and a long time for the impregnation of the resin. In contrast, the reactive processing requires relatively low temperature.⁹⁹ In addition, low viscosity enables vacuum infusion. Many of the thermoplastics dissolve in their monomer.⁴⁰ By adjusting the amount of the predissolved polymer in the monomer, the viscosity of the initial resin can be adjusted. Recently, an acrylic-based material called Elium has been commercially available.^{95,100,101} When composites are fabricated using thermoplastics, the fiber and the polymer can be recovered by dissolution, as is demonstrated in Fig. 10.¹⁰² The economic factor for the composite recycling is also discussed.^{102–104}

6. Summary and future outlook

In this review, we summarized the recent advancements in understanding bulk polymerization, especially when the final product is a glassy solid. In this case, bulk polymerization can be seen as a process of polymerization-induced vitrification. Classically, less attention has been paid to the changes in the amorphous structure and physical properties during bulk polymerization. However, recent findings suggest the importance of considering these changes upon polymerization-induced vitrification. During bulk polymerization, a sudden reaction acceleration known as the Trommsdorff effect may occur, which has been attributed to the decreased termination



Fig. 9 Viscosity as a function of processing temperature. Controlling the viscosity of the resin is a critical factor in the fabrication of fiber-reinforced plastics. Reproduced from ref. 21 with permission from Elsevier, *Composites, Part A*, 2007, **38**, 666–681, copyright 2007.



rate because of increased viscosity. Recent studies also suggest a connection between this effect and apparent phase separation (*i.e.*, heterogeneity). When bulk polymerization is locally initiated and the reacting front propagates, this type of polymerization is termed frontal polymerization. While this technique has a long research history, the recent development of FROMP using norbornene derivatives significantly expands its potential applications. Bulk polymerization can also be applied in resin for fiber-reinforced plastics and additive manufacturing. In contrast, less attention has been paid to the pre-exponential frequency factor. It is increasingly suggested that changes in this frequency factor play a key role in causing sudden reaction acceleration. Phase separation may increase the frequency factor of one elementary reaction while decreasing that of another. For example, while the termination rate decreases, the propagation rate may increase in cases of phase separation.

Another important aspect is polymerization-induced vitrification. It has been established that the physical properties of glass are closely linked to its fragility, suggesting that resins may also be categorized according to their vitrification behavior. Recent studies have also emphasized the importance of changes in amorphous structure during polymerization. In frontal polymerization, an interface exists between the already cured glassy region (*i.e.*, the reacting front) and the liquid monomer phase, and controlling the amorphous structure at this interface may be important for stabilizing front propagation. Reaction-induced concentration gradients may also generate convective transport phenomena such as Marangoni-type flows. However, a detailed discussion of such flow-driven effects is beyond the scope of the present review, which focuses on bulk polymerization, vitrification, heterogeneity, and sudden reaction acceleration. Viewing bulk polymerization as a spatially heterogeneous and self-organizing process rather than a purely homogeneous reaction may provide new insights into how polymerization can be designed, monitored, and controlled. Extending such studies to a broader range of bulk polymerizations may help clarify how general sudden reaction acceleration is and whether similar kinetic phenomena emerge in other monomer systems.

Conflicts of interest

There are no conflicts to declare.

Data availability

This review article does not report new experimental or simulation data. All data discussed are available in the cited literature.

Acknowledgements

Y. S. acknowledges financial support from JSPS KAKENHI (Grant No. 25K07245).

References

- 1 P. J. Flory, *Principles of polymer chemistry*, Cornell University Press, Ithaca, NY, 1953.
- 2 T. P. Lodge and P. C. Hiemenz, *Polymer chemistry: International student edition*, CRC Press, Boca Raton, FL, 3rd edn, 2021.
- 3 R. J. Young and P. A. Lovell, *Introduction to Polymers*, CRC Press, Boca Raton, FL, 3rd edn, 2011.
- 4 J. M. Nölle, S. Primpke, K. Müllen, P. Vana and D. Wöll, *Polym. Chem.*, 2016, **7**, 4100–4105.
- 5 D. Wöll, E. Braeken, A. Deres, F. C. De Schryver, H. Uji-i and J. Hofkens, *Chem. Soc. Rev.*, 2009, **38**, 313–328.
- 6 B. Stempfle, M. Dill, M. Winterhalder, K. Müllen and D. Wöll, *Polym. Chem.*, 2012, **3**, 2456–2463.
- 7 D. Wöll, *RSC Adv.*, 2014, **4**, 2447–2465.
- 8 Y. Suzuki, Y. Shinagawa, E. Kato, R. Mishima, K. Fukao and A. Matsumoto, *Macromolecules*, 2021, **54**, 3293–3303.
- 9 Y. Suzuki, D. S. Cousins, Y. Shinagawa, R. T. Bell, A. Matsumoto and A. P. Stebner, *Polym. J.*, 2019, **51**, 423–431.
- 10 C. P. Brangwynne, C. R. Eckmann, D. S. Courson, A. Rybarska, C. Hoegge, J. Gharakhani, F. Jülicher and A. A. Hyman, *Science*, 2009, **324**, 1729–1732.
- 11 I. D. Robertson, M. Yourdkhani, P. Centellas, J. E. Aw, D. Ivanoff, E. Goli, E. M. Lloyd, L. M. Dean, N. Sottos, P. Geubelle, J. S. Moore and S. White, *Nature*, 2018, **557**, 223–227.
- 12 B. A. Suslick, J. Hemmer, B. R. Groce, K. J. Stawiasz, P. H. Geubelle, G. Malucelli, A. Mariani, J. S. Moore, J. A. Pojman and N. R. Sottos, *Chem. Rev.*, 2023, **123**, 3237–3298.
- 13 H. Galina, K. Dušek, Z. Tuzar, M. Bohdanecky and J. Štokr, *Eur. Polym. J.*, 1980, **16**, 1043–1046.
- 14 K. Dušek, *Br. Polym. J.*, 1985, **17**, 185–189.
- 15 J. E. Elliott and C. N. Bowman, *Macromolecules*, 1999, **32**, 8621–8628.
- 16 C. N. Bowman and C. J. Kloxin, *AIChE J.*, 2008, **54**, 2775–2795.
- 17 Y. Suzuki, R. Mishima and A. Matsumoto, *Int. J. Chem. Kinet.*, 2022, **54**, 361–370.
- 18 J. J. Keating IV and J. L. Plawsky, *Macromolecules*, 2020, **53**, 7224–7238.
- 19 *Polymer Handbook*, ed. J. Brandrup, E. H. Immergut and E. A. Grulke, Wiley-Interscience, 4th edn, 1999.
- 20 G. Odian, Reactions of Polymers, in *Principles of Polymerization*, John Wiley & Sons, Hoboken, NJ, 4th edn, 2004, pp. 729–788.
- 21 K. van Rijswijk and H. E. N. Bersee, *Composites, Part A*, 2007, **38**, 666–681.
- 22 F.-L. Jin, X. Li and S.-J. Park, *J. Ind. Eng. Chem.*, 2015, **29**, 1–11.
- 23 J. J. Chruściel and E. Leśniak, *Prog. Polym. Sci.*, 2015, **41**, 67–121.



- 24 M. R. Buchmeiser, in *Handbook of Ring-Opening Polymerization*, Wiley-VCH Verlag GmbH & Co. KGaA, Weinheim, Germany, 2009, pp. 197–225.
- 25 B. M. Novak, W. Risse and R. H. Grubbs, in *Polymer Synthesis Oxidation Processes*, Springer Berlin Heidelberg, Berlin, Heidelberg, 1992, pp. 47–72.
- 26 N. Ide and T. Fukuda, *Macromolecules*, 1999, **32**, 95–99.
- 27 E. J. Juarez-Perez, M. Wußler, F. Fabregat-Santiago, K. Lakus-Wollny, E. Mankel, T. Mayer, W. Jaegermann and I. Mora-Sero, *J. Phys. Chem. Lett.*, 2014, **5**, 680–685.
- 28 G. A. O'Neil and J. M. Torkelson, *Macromolecules*, 1999, **32**, 411–422.
- 29 Q. Tran-Cong-Miyata, T. Kinohira, D.-T. Van-Pham, A. Hirose, T. Norisuye and H. Nakanishi, *Curr. Opin. Solid State Mater. Sci.*, 2011, **15**, 254–261.
- 30 T. Ozaki, T. Koto, T. V. Nguyen, H. Nakanishi, T. Norisuye and Q. Tran-Cong-Miyata, *Polymer*, 2014, **55**, 1809–1816.
- 31 C. P. Brangwynne, P. Tompa and R. V. Pappu, *Nat. Phys.*, 2015, **11**, 899–904.
- 32 M. Feric, N. Vaidya, T. S. Harmon, D. M. Mitrea, L. Zhu, T. M. Richardson, R. W. Kriwacki, R. V. Pappu and C. P. Brangwynne, *Cell*, 2016, **165**, 1686–1697.
- 33 Y. Shin and C. P. Brangwynne, *Science*, 2017, **357**, eaaf4382.
- 34 Y. Suzuki, Y. Doi, R. Mishima, K. Mayumi and A. Matsumoto, *Macromolecules*, 2023, **56**, 3731–3738.
- 35 L. Berthier and M. D. Ediger, *Phys. Today*, 2016, **69**, 40–46.
- 36 P. W. Anderson, *Science*, 1995, **267**, 1615.
- 37 M. D. Ediger, *Annu. Rev. Phys. Chem.*, 2000, **51**, 99–128.
- 38 J. Mattsson, H. M. Wyss, A. Fernandez-Nieves, K. Miyazaki, Z. Hu, D. R. Reichman and D. A. Weitz, *Nature*, 2009, **462**, 83–86.
- 39 L. Tsapatsaris, L. Wiegart, S. Petrash, A. Ribbe, J. Cash, T. Engels, M. Endoh and T. Koga, *Macromolecules*, 2025, **58**, 8079–8090.
- 40 B. A. Miller-Chou and J. L. Koenig, *Prog. Polym. Sci.*, 2003, **28**, 1223–1270.
- 41 J. Keddie, *Mater. Sci. Eng., R*, 1997, **21**, 101–170.
- 42 Y. Suzuki, *Polym. J.*, 2023, **55**, 807–815.
- 43 Y. Suzuki, R. Mishima, E. Kato and A. Matsumoto, *Polym. J.*, 2023, **55**, 229–238.
- 44 C. A. Angell, *Science*, 1995, **267**, 1924–1935.
- 45 M. D. Ediger, C. A. Angell and S. R. Nagel, *J. Phys. Chem.*, 1996, **100**, 13200–13212.
- 46 P. G. Debenedetti and F. H. Stillinger, *Nature*, 2001, **410**, 259.
- 47 R. Lovell, G. R. Mitchell and A. H. Windle, *Faraday Discuss. Chem. Soc.*, 1979, **68**, 46–57.
- 48 G. R. Mitchell and A. H. Windle, *Polymer*, 1984, **25**, 906–920.
- 49 Y. Suzuki, R. Mishima, S. Onozato, J.-C. Tseng, S. Hiroi, K. Kobayashi, K. Ohara and A. Matsumoto, *Polym. J.*, 2024, **56**, 1005–1015.
- 50 Q. Tran-Cong-Miyata and H. Nakanishi, *Polym. Int.*, 2017, **66**, 213–222.
- 51 R. G. W. Norrish and E. F. Brookman, *Proc. R. Soc. London*, 1939, **171**, 147–171.
- 52 R. G. W. Norrish and R. R. Smith, *Nature*, 1942, **150**, 336–337.
- 53 V. E. Trommsdorff, H. Köhle and P. Lagally, *Makromol. Chem.*, 1948, **1**, 169–198.
- 54 V. G. V. Schulz and G. Harborth, *Makromol. Chem.*, 1947, **1**, 106–139.
- 55 M. S. Matheson, E. E. Auer, E. B. Bevilacqua and E. J. Hart, *J. Am. Chem. Soc.*, 1949, **71**, 497–504.
- 56 M. S. Matheson, E. E. Auer, E. B. Bevilacqua and E. J. Hart, *J. Am. Chem. Soc.*, 1951, **73**, 5395–5400.
- 57 *Radicals in organic synthesis*, ed. M. P. S. Philippe Renaud, Wiley-VCH, Weinheim, Germany, 2008.
- 58 K. Matyjaszewski, *Handbook of radical polymerization*, John Wiley & Sons, Chichester, England, 2003.
- 59 P. Hayden and H. Melville, *J. Polym. Sci.*, 1960, **43**, 201–214.
- 60 R. Sack, G. V. Schulz and G. Meyerhoff, *Macromolecules*, 1988, **21**, 3345–3352.
- 61 P. B. Zetterlund, H. Yamazoe and B. Yamada, *Polymer*, 2002, **43**, 7027–7035.
- 62 C. Barner-Kowollik and G. T. Russell, *Prog. Polym. Sci.*, 2009, **34**, 1211–1259.
- 63 J. Barth, M. Buback, G. T. Russell and S. Smolne, *Macromol. Chem. Phys.*, 2011, **212**, 1366–1378.
- 64 T. J. Tulig and M. Tirrell, *Macromolecules*, 1981, **14**, 1501–1511.
- 65 P. G. de Gennes, *J. Chem. Phys.*, 1971, **55**, 572–579.
- 66 M. Doi and S. F. Edwards, *J. Chem. Soc., Faraday Trans. 2*, 1978, **74**, 1789–1801.
- 67 G. A. O'Neil, M. B. Wisnudel and J. M. Torkelson, *Macromolecules*, 1996, **29**, 7477–7490.
- 68 G. Johnston-Hall and M. J. Monteiro, *Macromolecules*, 2008, **41**, 727–736.
- 69 D. S. Achilias and C. Kiparissides, *Macromolecules*, 1992, **25**, 3739–3750.
- 70 D. S. Achilias and I. D. Sideridou, *Macromolecules*, 2004, **37**, 4254–4265.
- 71 A. Zoller, D. Gimes and Y. Guillaneuf, *Polym. Chem.*, 2015, **6**, 5719–5727.
- 72 D. S. Achilias, *Macromol. Theory Simul.*, 2007, **16**, 319–347.
- 73 T. J. Tulig and M. Tirrell, *Macromolecules*, 1982, **15**, 459–463.
- 74 G. A. O'Neil, M. B. Wisnudel and J. M. Torkelson, *AIChE J.*, 1998, **44**, 1226–1231.
- 75 E.-H. P. Wolff and A. N. R. Bos, *Ind. Eng. Chem. Res.*, 1997, **36**, 1163–1170.
- 76 G. Odian, T. Acker and M. Sobel, *J. Appl. Polym. Sci.*, 1963, **7**, 245–250.
- 77 N. Mori, A. Matsumoto and Y. Suzuki, *Macromolecules*, 2025, **58**, 4699–4707.
- 78 E. Sasaki, K. Kobayashi, Y. Doi, T. Oda, K. Mayumi, K. Ohara, A. Matsumoto and Y. Suzuki, *Macromolecules*, 2025, **58**, 6624–6633.
- 79 V. B. Golubev, D. G. Gromov and B. A. Korolev, *J. Appl. Polym. Sci.*, 1992, **46**, 1501–1502.



- 80 A. G. West, C. Barner-Kowollik and S. Perrier, *Polymer*, 2010, **51**, 3836–3842.
- 81 Y. Suzuki, S. Onozato, Y. Shinagawa and A. Matsumoto, *ACS Omega*, 2022, **7**, 38933–38941.
- 82 S. Onozato, C. Kojima, A. Matsumoto and Y. Suzuki, *Macromol. Chem. Phys.*, 2024, **225**, 2400147.
- 83 L. L. Lewis, C. S. DeBisschop, J. A. Pojman and V. A. Volpert, *J. Polym. Sci., Part A: Polym. Chem.*, 2005, **43**, 5774–5786.
- 84 J. A. Pojman, *J. Am. Chem. Soc.*, 1991, **113**, 6284–6286.
- 85 N. M. Chechilo, R. Y. Khvilivitskii and N. S. Enikolopyan, *Dokl. Akad. Nauk SSSR*, 1972, **204**, 1180–1181.
- 86 N. M. Chechilo and N. S. Enikolopyan, *Dokl. Phys. Chem.*, 1974, **214**, 174–176.
- 87 N. M. Chechilo and N. S. Enikolopyan, *Dokl. Phys. Chem.*, 1975, **221**, 392–394.
- 88 Y. Koike, Y. Takezawa and Y. Ohtsuka, *Appl. Opt.*, 1988, **27**, 486–491.
- 89 Y. Koike, E. Nihel, N. Tanio and Y. Ohtsuka, *Appl. Opt.*, 1990, **29**, 2686–2691.
- 90 V. V. Ivanov, E. V. Stegno and L. M. Pushchaeva, *Chem. Phys. Rep.*, 1997, **16**, 947–951.
- 91 V. V. Ivanov, E. V. Stegno and L. M. Pushchaeva, *Polym. Sci., Ser. A*, 2002, **44**, 1017–1022.
- 92 V. V. Ivanov, V. P. Mel'nikov and E. V. Stegno, *Russ. J. Phys. Chem. B*, 2012, **6**, 750–751.
- 93 S. I. Evstratova, D. Antrim, C. Fillingane and J. A. Pojman, *J. Polym. Sci., Part A: Polym. Chem.*, 2006, **44**, 3601–3608.
- 94 Q. Z. Yan, G. D. Lu, W. F. Zhang, X. H. Ma and C. C. Ge, *Adv. Funct. Mater.*, 2007, **17**, 3355–3362.
- 95 S. K. Bhudolia, G. Gohel, K. F. Leong and S. C. Joshi, *Composites, Part B*, 2020, **203**, 108480.
- 96 S.-S. Yao, F.-L. Jin, K. Y. Rhee, D. Hui and S.-J. Park, *Composites, Part B*, 2018, **142**, 241–250.
- 97 C. E. Bakis, L. C. Bank, V. L. Brown, E. Cosenza, J. F. Davalos, J. J. Lesko, A. Machida, S. H. Rizkalla and T. C. Triantafillou, *J. Compos. Constr.*, 2002, **6**, 73–87.
- 98 R. Mahshid, M. N. Isfahani, M. Heidari-Rarani and M. Mirkhalaf, *Composites, Part A*, 2023, **171**, 107584.
- 99 Y. Suzuki, D. Cousins, J. Wassgren, B. B. Kappes, J. Dorgan and A. P. Stebner, *Composites, Part A*, 2018, **104**, 60–67.
- 100 L. C. M. Barbosa, D. B. Bortoluzzi and A. C. Ancelotti Jr, *Composites, Part B*, 2019, **175**, 107082.
- 101 M. E. Kazemi, L. Shanmugam, D. Lu, X. Wang, B. Wang and J. Yang, *Composites, Part A*, 2019, **125**, 105523.
- 102 D. S. Cousins, Y. Suzuki, R. E. Murray, J. R. Samaniuk and A. P. Stebner, *J. Cleaner Prod.*, 2019, **209**, 1252–1263.
- 103 J. Zhang, V. Chevali, H. Wang and C.-H. Wang, *Composites, Part B*, 2020, **193**, 108053.
- 104 G. Oliveux, L. Dandy and G. Leeke, *Prog. Mater. Sci.*, 2015, **72**, 61–99.

